protons play a role in relaxing the ^{113}Cd nucleus. This selective NOE experiment also demonstrates that spin diffusion is an ineffective mechanism for transferring spin polarization from the water or methine protons to the acetate methylene protons, as no change in the ^{113}Cd resonance intensity was observed when the water or methine protons were selectively irradiated.

The absence of a dipole–dipole contribution to ^{113}Cd relaxation from water protons in aqueous CdCyDTA solutions is in contrast to the results obtained for CdEDTA solutions[6] and suggests that little or no water is present in the CdCyDTA coordination sphere. Thus the CyDTA ligand must be six-coordinate for virtually all of the time.

Also, the absence of a dipole–dipole contribution to ^{113}Cd relaxation from the methine protons of CyDTA would seem to suggest that the methine protons are significantly farther away from the Cd nucleus than are the acetate methylene protons, as dipolar relaxation has a $1/r^6$ dependence. However, the molecular reorientation motion of CdCyDTA in solution may be anisotropic, in which case the correlation time that governs the ^{113}Cd–^1H(methine) dipole–dipole interaction could be different from the correlation time governing the ^{113}Cd–^1H(methylene) interaction. It is thus possible that a similar r_{H-Cd} but a shorter correlation time is responsible for the lack of involvement of the methine protons in the ^{113}Cd T_1^{DD}.

In fact, evidence exists that the methine protons and the axial in-plane acetate methylene protons are closer to the metal center than are other ligand protons; for example, in a ^1H NMR study of the paramagnetic NiCyDTA complex, no ^1H resonance was observed for either the methine protons or the axial in-plane methylene protons.[12] A reasonable explanation of the failure to observe the resonances is that these protons are closest to the Ni atom and that electron–nuclear dipole–dipole relaxation (which also has a $1/r^6$ dependence) greatly broadened the two types of proton resonances.

Acknowledgment. We gratefully acknowledge research support from the National Science Foundation.

Registry No. $CdCyDTA^{2-}$, 12607-87-3.

(12) Erickson, L. E.; Young, D. C.; Ho, F. F.-L.; Watkins, S. R.; Terrill, J. B.; Reilley, C. N. *Inorg. Chem.* **1971**, *10*, 441–453.

Electronic Structure of Bis(pentadienyl)iron. Semiempirical Calculations and Photoelectron Spectra[1,2]

Michael C. Böhm,[3] Mirjana Eckert-Maksić,[3] Richard D. Ernst,*[4] David R. Wilson,[4] and Rolf Gleiter*[3]

Contribution from the Institut für Organische Chemie der Universität Heidelberg, D-6900 Heidelberg, West Germany, and the Department of Chemistry, University of Utah, Salt Lake City, Utah 84112. *Received August 3, 1981*

Abstract: The electronic structure of dipentadienyliron (**1**) and its methyl derivatives **2** to **4** has been investigated by means of semiempirical LCAO calculations of the INDO and charge-iterative extended Hückel (EH) types as well as by means of their He I photoelectron (PE) spectra. A significant rotational barrier in the open ferrocenes is predicted, and the origin of the preference of the trans C_{2h} conformation in the gas phase is analyzed. The electronic structure of the bis(pentadienyl) complexes is compared with the nature of bonding in ferrocene and the bis(diene)iron monocarbonyl species. In the open systems a very large degree of metal–ligand coupling and as a result of a larger flexibility of the 3d basis functions a bonding interaction of partial δ character is observed; this behavior is not encountered in ferrocene. In the PE spectra of **2**–**4** two Fe 3d ionization events are predicted on top of the complex HOMO derived from the nonbonding pentadienyl orbitals.

Recently dipentadienyliron (**1**) and several methyl derivatives (e.g., **2**–**4**) have been synthesized.[5] It has been demonstrated that

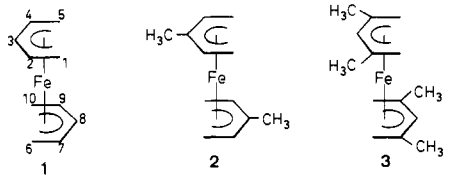

1 **2** **3**

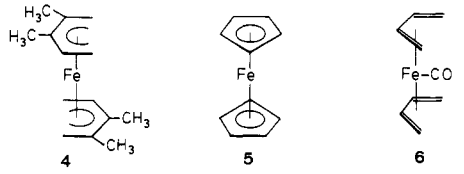

4 **5** **6**

the bis(pentadienyl)iron systems are η^5 complexes with similar iron–carbon distances as in the cyclic counterpart ferrocene (**5**).

The electronic structure of the closed sandwich ferrocene has been the subject of various theoretical publications. The degree of sophistication extends from semiempirical calculations of the Wolfsberg–Helmholtz type[6-8] to ab initio calculations of double-ζ quality.[9,10] Quantum chemical studies on bis(pentadienyl) complexes, on the other hand, are missing although various bis(π-allyl) systems theoretically have been analyzed in great detail.[11-13] In connection with our investigations on the dimeric ferrocene species[14] and the bis(diene)iron monocarbonyl systems[15] we be-

(1) Part 18 in the series. Electronic Structure of Organometallic Compounds. Part 17, see ref 2.

(2) M. C. Böhm, M. Eckert-Maksić, R. Gleiter, G. E. Herberich, and B. Hessner, *Chem. Ber.*, **115**, 754 (1982).

(3) Institut für Organische Chemie der Universität Heidelberg.

(4) Department of Chemistry, University of Utah.

(5) D. R. Wilson, A. A. Dilullo, and R. D. Ernst, *J. Am. Chem. Soc.*, **102**, 5928 (1980).

(6) R. D. Fischer, *Theor. Chim. Acta*, **1**, 418 (1963); J. H. Schachtschneider, R. Prins, and P. Roos, *Inorg. Chim. Acta*, **1**, 462 (1967); E. M. Shustorovich and M. E. Dyatkina, *Dokl. Phys. Chem. (Engl. Transl.)*, **128**, 885 (1959).

(7) J. W. Lauher and R. Hoffmann, *J. Am. Chem. Soc.*, **98**, 1729 (1976).

(8) J. H. Ammeter, H.-B. Bürgi, J. C. Thibeault, and R. Hoffmann, *J. Am. Chem. Soc.*, **100**, 3686 (1978).

(9) M.-M. Coutière, J. Demuynck, and A. Veillard, *Theor. Chim. Acta*, **27**, 281 (1972).

(10) P. S. Bagus, U. I. Wahlgren, and J. Almlöf, *J. Chem. Phys.*, **64**, 2324 (1976).

(11) A. D. Brown and A. Owens, *Inorg. Chim. Acta*, **5**, 675 (1971).

(12) A. Veillard, *J. Chem. Soc. D*, 1022, 1427 (1969); M.-M. Rohmer and A. Veillard, *J. Chem. Soc., Chem. Commun.*, 250 (1973); M.-M. Rohmer, J. Demuynck, and A. Veillard, *Theor. Chim. Acta*, **36**, 93 (1974).

(13) M. C. Böhm, R. Gleiter, and C. D. Batich, *Helv. Chim. Acta*, **63**, 990 (1980).

(14) M. C. Böhm, R. Gleiter, F. Delgado-Pena, and D. O. Cowan, *Inorg. Chem.*, **19**, 1081 (1980); M. C. Böhm and R. Gleiter, in preparation.

0002-7863/82/1504-2699$01.25/0

came interested in the electronic structure of "open ferrocenes" **1–4**.

In the present publication we try to develop a MO picture of bis(pentadienyl)iron derivatives which allows an understanding of the bonding capabilities, the rotational barriers, and the photoelectron (PE) spectra in the outer valence region of these compounds. The computational framework of our study is a recently developed INDO model for transition-metal compounds[16] and charge-iterative calculations[17] within the extended Hückel (EH) method.[18]

To assign PE spectra of transition-metal compounds theoretically, it must be taken into account that orbital reorganization effects are of significant importance in the case of ionization events from orbitals predominantly localized at the 3d center. The ordering of the ionic states differs from the MO sequence predicted for the electronic ground state.[19] Koopmans' theorem[20] ($I_{v_j}^{K} = -\epsilon_j$), which relates the vertical ionization potentials to the orbital energies, ϵ_j, of the N-electron system (e.g. the ground state), is not valid. To take into account both relaxation and correlation effects accompanying the ionization events, we have applied Green's function approach based on the many-body perturbation theory[21,22] for the interpretation of the PE spectra in the lower energy region.

Computational Methods

For the investigation of the electronic structure of the "open ferrocenes" and for the calculation of the ionization potentials we have used an INDO Hamiltonian designed to reproduce the results of ab initio calculations with larger basis sets (double-ζ quality) and to predict experimental observables (e.g., geometries, dipole moments, ionization potentials, excitation energies) with sufficient accuracy.[16] The predictive capability of the semiempirical Hamiltonian parametrized within the ZDO approximation has been demonstrated in various applications with transition-metal compounds. Ionization potentials of 3d complexes have been calculated by means of the ΔSCF and "transition operator" (TO) method[13-15,23] and within the many-body Green's function approach beyond the independent particle picture.[24] Often the accuracy of the INDO results have exceeded the predictive success of ab initio calculations. In ref 16 a detailed description of the INDO formalism is given.

On the other hand it is well-known that all semiempirical procedures based on the ZDO approximation have inherent shortcomings in predicting reliable energy differences between possible molecular conformations in those systems where the interaction between occupied fragment orbitals has a pronounced influence upon the equilibrium geometry.[25] For the study of geometrical preferences (the mutual orientation of the pentadienyl ligands) in the "open ferrocenes" we have used the charge-iterative extended Hückel (EH) procedure.[17,18] The validity of this method for the calculation of rotational barriers and overlap controlled coordination patterns in transition-metal compounds has been documented in recent years.[26,27]

Table I. Orbital Exponents (ζ) and Diagonal Elements H_{ii} for the EH Calculations on **1**

		ζ	H_{ii}, eV
Fe	4s	1.575	−9.64
	4p	0.975	−6.05
	3d	5.350 (0.53659) 1.800 (0.66779)	−11.27
C	2s	1.550	−20.14
	2p	1.325	−10.34
H	1s	1.300	−12.76

In the charge-iterative EH calculations the diagonal elements of the EH Hamiltonian were approximated by the quadratic from (1), where Q is the atomic charge. The parameters A, B, and C

$$H_{ii} = -I_i(Q) = AQ^2 + BQ + C \quad (1)$$

determine the charge dependence of H_{ii} and were taken from ref 28. For the off-diagonal elements the weighted H_{ij} formula (2)

$$H_{ij} = K(S_{ij}|2)[(1 + \Delta)H_{ii} + (1 - \Delta)H_{jj}] \quad (2)$$

$$\Delta = \frac{H_{ii} - H_{jj}}{H_{ii} + H_{jj}} \quad (3)$$

has been used.[8] Here, S_{ij} stands for the overlap integral between the ith and the jth AO and K is the Wolfsberg-Helmholtz constant ($K = 1.75$). Charge-iterative calculations were performed for the cis (C_{2v}) and trans (C_{2h}) conformations of **1**; the observed H_{ii} values were then averaged.

Burns exponents[29] were used for C(2s,2p) and for 4s, 4p of the Fe center. For Fe 3d the double-ζ orbital exponents of Richardson and co-workers[30] have been selected while the semiempirical standard value 1.300 corresponds to the H 1s exponent. The orbital exponents as well as the various diagonal elements of the EH matrix are collected in Table I.

For the INDO and EH calculations geometrical parameters from X-ray data have been used.[5] The iron–carbon distances in **3** are 2.084 Å for the central C atoms, 2.074 Å for the 2,4 position, and the largest for the terminal FeC bond (2.114 Å). These separations slightly exceed the iron–carbon distance in ferrocene (2.033 Å).[31,32] The X-ray investigation on **3** has shown that the both pentadienyl ligands are oriented in a gauche-eclipsed conformation: the two ligand planes are weakly tilted in the direction of the Fe center (the dihedral angle between the two C_7H_{11} planes of **3** equals 15.01°). To reduce the geometrical degrees of freedom in the study of the rotational barrier of **1**, a planar orientation of the π ligands has been assumed.

Green's Function Formalism

The theoretical background of Green's function formalism has been derived in various references.[21,22,33,34] Therefore only a short outline of the method and the used approximations within the semiempirical INDO Hamiltonian is given.

The one-particle Green's function G in the Heisenberg picture is defined by means of eq 4.[34] In (4) $\langle\Psi_0^N|$ symbolizes the exact

(15) M. C. Böhm and R. Gleiter, *Chem. Ber.*, **113**, 3647 (1980).
(16) M. C. Böhm and R. Gleiter, *Theor. Chim. Acta*, **59**, 127 (1981).
(17) M. Zerner and M. Gouterman, *Theor. Chim. Acta*, **4**, 44 (1966); *ibid.*, **6**, 363 (1966); F. A. Cotton and C. B. Harris, *Inorg. Chem.*, **6**, 369 (1967); R. F. Fenske, K. G. Caulton, D. G. Radtke, and C. C. Sweeney, *ibid.*, **5**, 951 (1966); R. M. Canadine and I. H. Hillier, *J. Chem. Phys.*, **50**, 2984 (1969).
(18) R. Hoffmann, *J. Chem. Phys.*, **39**, 1397 (1963); R. Hoffmann and W. N. Lipscomb, *ibid.*, **36**, 2179 3489 (1962); **37**, 2872 (1962).
(19) A. Veillard and J. Demuynck, *Mod. Theor. Chem.*, **4**, (1977).
(20) T. Koopmans, *Physica (Amsterdam)*, **1**, 104 (1934).
(21) F. Ecker and G. Hohlneicher, *Theor. Chim. Acta*, **25**, 289 (1972). G. Hohlneicher, F. Ecker, and L. S. Cederbaum in "Electron Spectroscopy", D. E. Shirley, Ed., North Holland Publishing Co., Amsterdam, 1972. P. O. Nerbrant, *Int. J. Quantum Chem.*, **9**, 901 (1975).
(22) L. S. Cederbaum and W. Domcke, *Adv. Chem. Phys.*, **36**, 205 (1977).
(23) M. C. Böhm and R. Gleiter, Z. Naturforsch., *34b*, 1028 (1980); M. C. Böhm, J. Daub, R. Gleiter, P. Hofmann, M. F. Lappert, and K. Öfele, *Chem. Ber.*, **113**, 3629 (1980); M. C. Böhm and R. Gleiter, *Comput. Chem.*, **1**, 407 (1980).
(24) M. C. Böhm and R. Gleiter, *Theor. Chim. Acta*, **57**, 315 (1980).
(25) P. Caramella, K. N. Houk, and L. N. Domelsmith, *J. Am. Chem. Soc.*, **99**, 4511 (1977).
(26) T. A. Albright, P. Hofmann, and R. Hoffmann, *J. Am. Chem. Soc.*, **99**, 7546 (1977); T. A. Albright and R. Hoffmann, *Chem. Ber.*, **111**, 1578 (1978); T. A. Albright, R. Hoffmann, and P. Hofmann, *ibid.*, **111**, 1591 (1978).
(27) R. Hoffmann, T. A. Albright, and D. L. Thorn, *Pure Appl. Chem.*, **4**, 257 (1977) and references cited therein: R. Hoffmann, *Science (Washington, DC)*, **211**, 995 (1981) and references cited therein.
(28) S. P. McGlynn, L. G. Vanquickenborne, M. Kinoshita, and D. G. Carroll, "Introduction to Applied Quantum Chemistry", Holt, Rinehart and Winston, New York, 1972.
(29) G. Burns, *J. Chem. Phys.*, **41**, 1521 (1964).
(30) J. W. Richardson, W. C. Nieuwpoort, R. R. Powell, and W. F. Edgell, *J. Chem. Phys.*, **36**, 1057 (1962).
(31) R. K. Bohn and A. Haaland, *J. Organomet. Chem.*, **5**, 470 (1966).
(32) P. Seiler and J. D. Dunitz, *Acta Crystallogr., Sect. B*, **B35**, 1068 (1979).
(33) R. D. Mattuck, "A Guide to Feynman Diagrams in Many-Body Problems", McGraw-Hill, New York, 1967; A. Abrikosov, L. Gorkov, and J. Dzyaloshinskii, "Quantum Field Theoretical Methods in Statistical Physics", Pergamon Press, Oxford, 1965.
(34) D. J. Thouless, "The Quantum Mechanics of Many-Body Systems", Academic Press, New York, 1961.

$$G_{ij}(t) = -i\langle \Psi_0^N | T a_i(t) a_j^+(t) | \Psi_0^N \rangle \quad (4)$$

ground state of the N-electron system, T is Wick's time-ordering operator, and $a_i(t)$ and $a_j^+(t)$ are the creation and destruction operators defined for an orthonormal set of Hartree–Fock (HF) spin orbitals.

$$a_i(t) = \epsilon^{iHt} a_i e^{-iHt} \quad (5)$$

H stands for the Hamilton operator. The Fourier transform (6) of G in the Heisenberg representation (eq 5) has negative poles

$$G_{ij}(\omega) = \int_{-\infty}^{\infty} G_{ij}(t) e^{i\omega t}\, dt \quad (6)$$

whose real parts are associated to the vertical ionization potentials of the N-electron system. The working relation for the spectral representation of G is the inverse Dyson equation[35] (7). To

$$G^{-1} = (G^0)^{-1} - \Sigma(\omega) \quad (7)$$

calculate vertical IP's by means of the inverse Dyson equation, one has to determine those ω values for which (7) has eigenvalues equal to zero. G^0 is the matrix of the free Green's function. If canonical HF orbitals are used as a starting point, $(G^0)^{-1}$ is given by eq 8 and thus (7) is simplified to (9). ϵ denotes the diagonal

$$(G^0)^{-1} = \omega I - \epsilon \quad (8)$$

$$(G)^{-1} = \omega I - \epsilon - \Sigma(\omega) \quad (9)$$

matrix of the canonical HF one-electron energies. and I stands for the unit matrix of proper size. $\Sigma(\omega)$ in (7) and (9) is the self-energy operator which can be expanded in a series corresponding to different orders of perturbation. In the basis of canonical HF orbitals the first-order term in the $\Sigma(\omega)$ expansion vanishes and $\Sigma(\omega)$ is given by eq 10. To determine the energy

$$\Sigma(\omega) = \Sigma^2(\omega) + \ldots + \Sigma^\infty(\omega) \quad (10)$$

coordinate ω, we have applied the same approximations as in a recent study.[24] In the expansion (10) a second-order approximation is used. it is assumed that G is diagonal and the ω values are calculated by means of a Taylor series expansion, (11), about the Koopmans' pole.[36]

$$\omega_j^{(2)} = \epsilon_j + \Sigma_{jj}^{(2)}(\epsilon_j)\left(1 - \frac{\partial}{\partial\omega}\Sigma_{jj}^{(2)}(\omega)_{\epsilon_j}\right)^{-1} \quad (11)$$

These approximations allow a straightforward evaluation of the zeros in the inverse Dyson equation even in the case of large molecules and they are part of most of Green's function calculations by means of semiempirical LCAO procedures.[36,37] The matrix elements of the self-energy operator within the INDO model for an atomic s, p, d basis have been evaluated in ref 24.

Ground-State Properties

The EH rotational barrier of **1** for the interconversion between the trans (C_{2h}) and cis (C_{2v}) conformations **1a** and **1b** is displayed

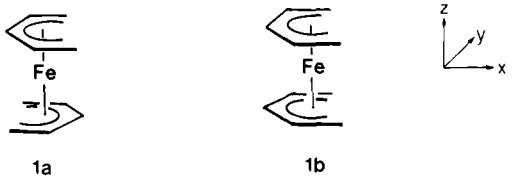

1a 1b

in Figure 1. According to the EH method the two extreme conformations **1a** and **1b** are separated by about 70 kJ/mol; the trans arrangement of the pentadienyl ligands corresponds to the minimum. INDO predicts an energy difference of 29 kJ/mol

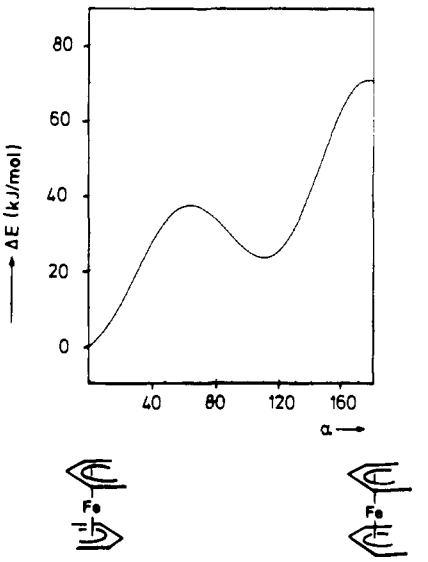

Figure 1. The calculated rotational barrier of dipentadienyliron (**1**) according to the EH procedure.

between both forms. A local minimum is found at $\alpha = 110°$, the energy gap between the trans conformation and the local minimum amounts to 22 kJ/mol according to the EH method. the $\alpha = 110°$ structure is close to the X-ray determined conformation (compound **3**) in the solid state which corresponds to a gauche-eclipsed orientation of the π-ligands. The solid-state geometry, however, is not only determined by intramolecular interactions; packing effects have a significant influence upon the molecular conformation in the crystal. The energy difference between the local and the absolute minimum is small enough that intermolecular packing forces might be able to determine the orientation of flexible molecular ribbons.[38] It should be pointed out that the relative minima correspond to an octahedral disposition of the carbon centers 1, 3, and 5, an orientation that is to be expected for a d^6 complex (formally Fe^{2+}). The relative maxima on the other hand have a trigonal-prismatic arrangement of C_1, C_3, and C_5. The prediction of a significant rotational barrier in open ferrocenes is supported by NMR data. The NMR spectrum of the bis(2,3-dimethylpentadienyl)iron complex (**4**) is in line with two nonsuperimposable isomers **4a** and **4b**. Due to the large

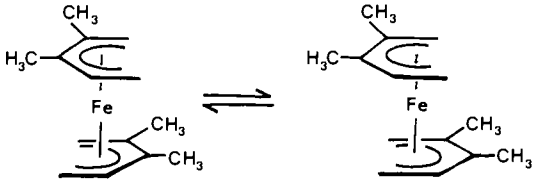

4a 4b

separation between the methyl groups at the pentadienyl ligands, comparable thermodynamic stabilities must be expected, a result that is supported by the semiempirical calculations. Therefore identical NMR spectra for the two isomers must be expected in the case of a low rotational barrier.

The conformational behavior of the open ferrocenes differs dramatically from the rotational barrier in **5**. In ferrocene the eclipsed D_{5h} and the staggered D_{5d} conformation are separated by an energy gap less than 4 kJ/mol (EH predicts 3.75 kJ/mol). The electronic factors determining the divergent properties of the open system **1** and ferrocene can be explained by means of α-dependent metal-to-ligand and ligand-to-metal charge-transfer interactions. In Figure 2 the Fe 3d atomic orbital populations[39] ($3d_{z^2}$, $3d_{xz}$, $3d_{yz}$, $3d_{x^2-y^2}$, and $3d_{xy}$) of **1** according to the EH

(35) F. J. Dyson, *Phys. Rev.*, **75**, 486 (1949).
(36) B. Kellerer, L. S. Cederbaum, and G. Hohlneicher, *J. Electron Spectrosc. Relat. Phenom.*, **3**, 107 (1974).
(37) S. Biskupic, L. Valko, and V. Kvasnicka, *Theor. Chim. Acta*, **38**, 149 (1975); P. Lazeratti and R. Zanasi, *Chem. Phys. Lett.*, **42**, 411 (1976); B. J. Duke and M. P. S. Collins, *ibid.*, **54**, 308 (1978); C.-M. Liegener and U. Scherz, *Theor. Chim. Acta*, **52**, 103 (1979); C.-M. Liegener, *ibid.*, **57**, 219 (1980).
(38) E. Huler and A. Warshel, *Acta Crystallogr. Sect. B*, **B30**, 1822 (1974); A. Warshel, E. Huler, D. Rabinovich, and Z. Shakked, *J. Mol. Struct.*, **23**, 175 (1974).
(39) R. S. Mulliken, *J. Chem. Phys.*, **23**, 1833, 2343 (1955).

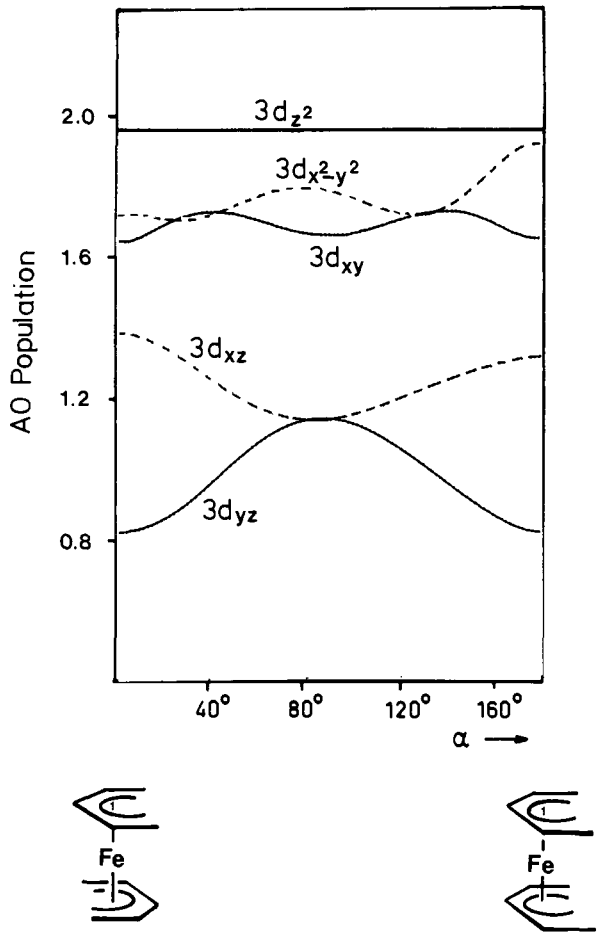

Figure 2. The AO population of the Fe 3d functions ($3d_{z^2}$, $3d_{xz}$, $3d_{yz}$, $3d_{x^2-y^2}$, and $3d_{xy}$) of **1** as function of the rotational angle α (EH procedure).

Table II. Comparison between the Fe 3d AO Populations of 1a and 1b According to the INDO and EH Methods

	trans (C_{2h})		cis (C_{2v})	
AO	INDO	EH	INDO	EH
$3d_{z^2}$	1.994	1.964	1.994	1.969
$3d_{xz}$	1.199	1.393	0.999	1.321
$3d_{yz}$	0.807	0.827	0.775	0.827
$3d_{x^2-y^2}$	1.663	1.716	1.965	1.917
$3d_{xy}$	1.665	1.656	1.637	1.655

calculation are shown as function of the rotational angle α. It is seen that $3d_{x^2-y^2}$ is depopulated in the case of C_{2h} symmetry (1.716 e) as a result of an efficient coupling with a ligand acceptor function. In the cis conformation the $3d_{x^2-y^2}$ population is raised up to 1.917 e. This metal-to-ligand interaction leading to a preference of the C_{2h} trans conformation is supported by an enhanced ligand-to-metal coupling; the population of $3d_{xz}$ is enlarged by the interconversion C_{2v} (cis) to C_{2h} (trans). According to EH the $3d_{xz}$ population is increased from 1.321 e (α = 180°) to 1.393 e (α = 0°). Figure 2 furthermore shows that the local minimum at α = 110° profits from the acceptor capability of both high-lying Fe 3d atomic orbitals, $3d_{xz}$ and $3d_{yz}$. The AO population of ($3d_{xz}$ + $3d_{yz}$) runs through a maximum at 110° (2.295 e) and is reduced at α = 0° (2.220 e) as well as in the cis form (2.148 e). The preference of the trans conformation therefore is determined by the metal-to-ligand coupling while ligand-to-metal charge transfer is most efficient in the gauche-eclipsed pentadienyl arrangement. The $3d_{z^2}$ and $3d_{xy}$ orbitals are not strongly influenced by the rotation of the pentadienyl moieties.

To support the EH-based argumentation, we have summarized in Table II the Fe 3d atomic orbital populations of the trans and cis forms **1a** and **1b** as calculated by means of the INDO and the EH methods. It is clearly seen that both procedures predict comparable variations in the 3d populations. The stabilization of the C_{2h} trans conformation (**1a**) unambiguously can be traced back to a depopulation of the $3d_{x^2-y^2}$ donor orbital and an enlarged occupation of the Fe $3d_{xz}$ acceptor orbital.

The α-dependent coupling strength between the 3d atomic orbitals of the transition-metal center and the orbitals of the organic π systems leads to different molecular orbital patterns for **1** under C_{2h} and C_{2v} symmetry. As the INDO procedure is used for the interpretation of the PE spectra, we want to discuss the molecular orbital schemes of **1a** and **1b** in the electronic ground state on the basis of this SCF model. In Table III and IV the highest occupied MO's of **1a** and **1b** are collected. In Figure 3

Table III. Orbital Energies, ϵ_i, MO Type and the Iron 3d Contribution to the MO's of the Trans Conformation 1a of Bis(pentadienyl)iron According to an INDO Calculation (P = Pentadienyl Ligand)

MO	Γ_i[a]	MO type	ϵ_i, eV	% Fe 3d
31	$8b_u$	π_3(P)	−8.17	0.0
30	$10a_g$	π_3(P), $3d_{xz}$ (bonding)	−10.56	38.4
29	$7b_g$	π_2(P), $3d_{xy}$, $3d_{yz}$	−10.62	45.3
28	$6a_u$	π_2(P)	−10.79	0.0
27	$9a_g$	$3d_{x^2-y^2}$, $3d_{z^2}$, π_5* (P)	−11.13	87.7
26	$8a_g$	$3d_{z^2}$, $3d_{x^2-y^2}$	−11.29	97.0
25	$6b_g$	$3d_{xy}$, $3d_{yz}$, π_2(P) (bonding)	−11.32	36.2
24	$7b_u$	π_1(P)	−11.43	0.0

[a] The numbering scheme of the irreducible representations corresponds to the valence electrons. Core electrons are not considered in the summation. The irreducible representations in **2**, **3**, and **4** are related to the MO's of **1**; for sake of clearness a common classification has been used.

Table IV. Orbital Energies, ϵ_i, MO Type and the Iron 3d Contribution to the MO's of the Cis Conformation 1b of Bis(pentadienyl)iron According to an INDO Calculation

MO	Γ_i[a]	MO type	ϵ_i, eV	% Fe 3d
31	$10a_1$	π_3(P), $3d_{x^2-y^2}$ (antibonding)	−8.61	22.5
30	$8b_2$	π_1(P), π_5(P), $3d_{xz}$	−9.08	21.8
29	$7b_1$	$3d_{xz}$, π_2(P) (antibonding)	−10.46	43.6
28	$6a_2$	π_2(P), $3d_{yz}$	−10.88	23.8
27	$7b_2$	π_1(P), $3d_{xz}$	−10.91	18.5
26	$9a_1$	$3d_{z^2}$	−10.97	97.3
25	$6b_1$	π_2(P), $3d_{xz}$ (bonding)	−11.31	30.9
23[b]	$8a_1$	$3d_{x^2-y^2}$, π_3(P) (bonding)	−11.52	63.5

[a] See legend at the bottom of Table III. [b] Between MO 25 and MO 23 a σ orbital has been omitted. C_2 axis = x axis; $\sigma_V = \sigma_{xy}$; $\sigma_V' = \sigma_{xz}$.

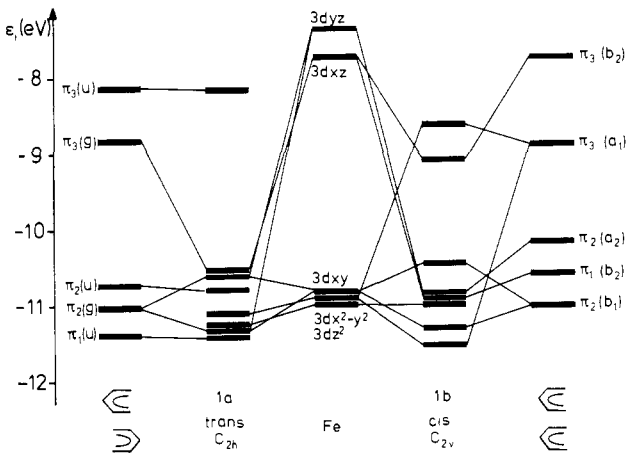

Figure 3. Interaction diagram between the iron 3d orbitals and the π functions of the pentadienyl ligands of **1** in the case of the trans (**1a**) and cis (**1b**) conformation. The Fe 3d orbitals are split as a result of the interaction with the σ frame of the organic ligands.

the most important interactions between the Fe 3d AO's and the ligand π orbitals are displayed schematically. The destabilization of $3d_{xz}$ and $3d_{yz}$ is a result of the σ MO's of the pentadienyl moieties.

The highest occupied MO of **1a** is the ungerade linear combination of the nonbonding (π_3) π functions of the pentadienyl ligands.

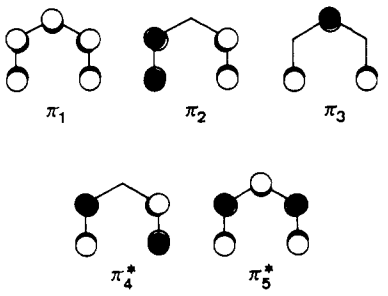

Due to symmetry the orbital $8b_u$ (−8.17 eV) contains no Fe 3d contributions. The next molecular orbital ($10a_g$) is the gerade linear combination of the nonbonding (π_3) fragment orbitals effectively stabilized by the $3d_{xz}$ acceptor function. The iron atomic orbitals contribute with 38.4% to the wave function.

$10a_g$ (−10.56 eV) is only 0.06 eV separated from another molecular orbital ($7b_g$) with significant Fe 3d contributions (45.3%). The ligand contribution corresponds to the in-phase combination of π_2; the predominant Fe 3d amplitude to the orbital wave function results from the $3d_{xy}$ atomic orbital. Due to some $3d_{yz}$ contribution, a tilting motion of the 3d orbitals takes place: the Fe 3d amplitude points in the directions of the central carbon centers, thus avoiding an antibonding interaction between the 3d components and the π fragments. The partner molecular orbital of $7b_g$ is predicted at −11.32 eV ($6b_g$). The Fe 3d character in $7b_g$ slightly exceeds the Fe amplitude in $6b_g$ (45.3% vs. 36.2%). As a result of a changed phase relation between $3d_{xy}$ and $3d_{yz}$, a rotation in the direction of the terminal C atoms is observed. The $3d_{yz}$ contributions to $6b_g$ and $7b_g$ therefore allow an in-phase coupling between the iron and ligand functions in both molecular orbitals.

The strong interaction between Fe $3d_{xy}$ and fragment molecular orbitals of the ligands is responsible for differences in the electronic structure of **1a** and ferrocene. In the cyclic complex $3d_{xy}$ and $3d_{yz}$ belong to different irreducible representations. As a result of this discrimination an intense interaction between $3d_{xy}$ of the iron center and the ligand orbitals is prevented. $3d_{xy}$ and $3d_{x^2-y^2}$ form a degenerate e_2' (D_{5h}) or e_{2g}(D_{5d}) linear combination strongly localized at the 3d atom. According to the INDO model 90% Fe 3d character is calculated for the degenerate $3d_{x^2-y^2}/3d_{xy}$ molecular orbitals in ferrocene.

The interaction between $3d_{xy}$ and the pentadienyl fragment furthermore is enhanced by means of a rotation of the terminal CH_2 groups in a way that the π atomic orbitals point toward the Fe center. A schematical representation of this deformation is given below.

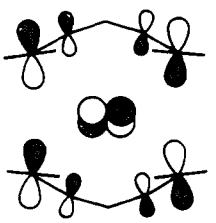

The tilt of the terminal CH_2 groups additionally minimizes the steric repulsion between the endo-H atoms at C_1 and C_5.

At −10.79 eV the second ungerade combination of the trans complex **1a** is predicted. This is the $6a_u$ antibonding linear combination of π_2. According to the INDO model an energy gap of 2.62 eV between the two π molecular orbitals of ungerade symmetry is predicted. Table III shows that the three closely spaced molecular orbitals $10a_g$, $7b_g$, and $6a_u$ (−10.56 eV to −10.79 eV) are separated by 0.34 eV from a set of orbitals ($9a_g$, $8a_g$, $6b_g$, and $7b_u$) in an energy interval of 0.3 eV.

The highest member of this second group is $9a_g$, predominantly of $3d_{x^2-y^2}$ character; $3d_{z^2}$ contributions allow a rotation into the direction of the central carbon atoms.

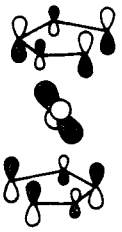

As a result of this tilting motion the interaction with the symmetry-adapted π_5^* combination is enlarged. The Fe 3d character of $9a_g$ amounts to 87.7%, of which 55.5% correspond to $3d_{x^2-y^2}$, the remaining being the $3d_{z^2}$ contribution. The mixing between $3d_{x^2-y^2}$ and $3d_{z^2}$ obviously allows a more efficient coupling between Fe functions and ligand acceptor orbitals leading to a stronger "δ bond" in comparison to ferrocene. This result is in line with recent Mössbauer investigations on the open ferrocences.[40] The classification into σ, π, and δ bonds in the case of the open ferrocenes in only a rough model, taking pattern from the "classical" description of metal–ligand coupling schemes. In a more sophisticated argumentation it is clear that the nature of the Fe ligand interaction lies between the idealized description (e.g., σ, π, and δ bonds) as σ-type and δ-type interactions are coupled in the high-lying valence orbitals.

$8a_g$ (−11.29 eV) is the orbital with the most pronounced localization (97%) at the iron center and is predominantly of $3d_{z^2}$ type. Of the two remaining molecular orbitals, $6b_g$ already has been mentioned. $7b_u$ at −11.43 eV corresponds to the out-of-phase linear combination of the lowest π orbital (π_1) of the C_5H_7 ligands.

In **1b** tilting deformations of the Fe 3d orbitals are prevented due to the mirror plane $\sigma_v = \sigma_{xy}$. The separation between the two highest occupied molecular orbitals ($10a_1$ and $8b_2$) is reduced to 0.47 eV. The HOMO of **1b** is the in-phase combination of π_3 with antibonding $3d_{x^2-y^2}$ contributions. The conformation-determining influence of $3d_{x^2-y^2}$ is clearly recognized. The $8b_2$ orbital contains contributions from the out-of-phase π_1 ligand orbital, from the π_5^* acceptor orbital, and from the $3d_{xz}$ orbital. $7b_1$ represents the destabilized linear combination between π_2 (in-phase) and Fe $3d_{xy}$. The bonding combination resulting from this interaction is found at −11.31 eV; $7b_1$ and $6b_1$ are separated by 0.85 eV. Table IV shows that $3d_{xy}$ dominates in $7b_1$ and is of minor importance in the $6b_1$ orbital. $6a_2$ is the out-of-phase linear combination of π_2 stabilized by means of the $3d_{yz}$ acceptor function. $7b_2$ contains large contributions from π_1 and from $3d_{xz}$.

The remaining molecular orbitals of **1b**, $9a_1$ and $8a_1$, show Fe 3d contributions that exceed 60%. $9a_1$ with 97.3% Fe $3d_{z^2}$ character shows negligible pentadienyl contributions, and $8a_1$ corresponds to the bonding combination between $3d_{x^2-y^2}$ and π_3 of the ligand fragment. The Fe 3d contribution (63.5%) clearly exceeds the ligand amplitude. However, in comparison with the $3d_{x^2-y^2}$ orbital in ferrocene and the $9a_g$ orbital of the trans complex a significant reduction of the Fe 3d contribution to the wave function is predicted.

The difference of the metal-to-ligand coupling in **1a** and **1b** is the result of more flexible Fe 3d functions under C_{2h} symmetry. The mixing between $3d_{xy}$ and $3d_{yz}$ as well as $3d_{x^2-y^2}$ and $3d_{z^2}$ allows a stronger interaction between donor and acceptor levels and leads to a reduction of the antibonding coupling between occupied fragment orbitals in the case of the trans conformation. The INDO results summarized in Tables III and IV indicate the existence of two molecular orbitals with large 3d amplitudes in **1a** ($8a_g$, $9a_g$). In **1b** only one orbital is strongly localized at the transition-metal center ($9a_1$). A similar pattern has been detected in the bis(butadiene)iron monocarbonyl complex (**6**).[15] **1a** lies

(40) R. H. Herber, private communication.

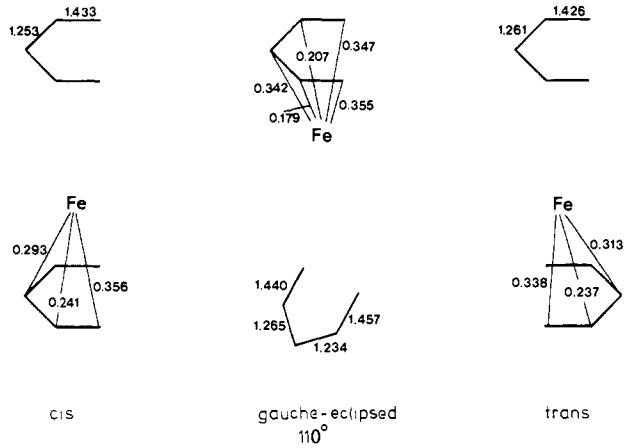

Figure 4. Wiberg indices of **1** in different conformations.

between the ferrocene case with three strongly localized molecular orbitals ($3d_{z^2}$, $3d_{x^2-y^2}$, $3d_{xy}$) on one side and **1b** or the monocarbonyl derivative **6** with a single localized Fe 3d atomic orbital on the other side. Below we have compared the INDO orbital energies of the frontier orbitals (HOMO/LUMO) of **1a** and of ferrocene (**5**).

	1a ϵ_i, eV		5 ϵ_i, eV	
LUMO	−0.74		−0.04	
		$\lvert\Delta\epsilon_i\rvert = 7.43$		$\lvert\Delta\epsilon_i\rvert = 9.87$
HOMO	−8.17		−9.91	

The smaller HOMO/LUMO gap in the open ferrocene is clearly recognized. In the case of the INDO MO approach the gauche conformation ($\alpha = 110°$) is 20.5 KJ/mol above the C_{2h} minimum; this energy difference is close to the calculated EH gap. Of course then the energetic separation between the cis (maximum) and gauche conformation in the INDO framework is smaller in comparison to the EH model.

In the $\alpha = 110°$ conformation there are additional degrees of freedom for the 3d AO's to be combined to the valence orbitals of the complex as a result of the lower molecular symmetry. The HOMO of the gauche conformation is predicted at −9.00 eV (INDO model) and contains significant Fe 3d amplitudes (21.7%). The next MO is found at −9.13 eV. Hence the energy gap between the two highest occupied orbitals is smallest in the gauche conformation. In analogy to **1b** these two MO's are separated by about 1.5 eV from MO 29 (−10.70 eV). The remaining MO's in the $\alpha = 110°$ orientation are also close to the MO properties of the cis model (ϵ_i values, localization properties). With exception of Fe $3d_{z^2}$ there is, however, a stronger mixing of Fe $3d_{x^2-y^2}$, $3d_{xy}$, $3d_{xz}$, and 3_{yz} in the complex MO's with predominant metal character.

In Figure 4 the calculated Wiberg bond indices[41] for **1a** and **1b** and for a conformation with $\alpha = 110°$ are displayed. Significant differences for the various iron–carbon interactions are predicted. The strongest metal–carbon bond is found in the case of the terminal C atoms C_1/C_5. Therefore in the absence of assistance from supplemental Lewis bases significant activation energies are expected for isomerization into η^3 or η^1 complexes, a reaction type of large importance in catalytic σ–π rearrangements of transition-metal compounds.[42] The weakening at the iron C_3 bond due to destabilizing interactions between occupied fragment orbitals for the cis form is clearly seen. In the π framework a bond alternation is predicted for which there is some structural evidence. The CC bond indices for the $\alpha = 110°$ conformation indicate necessary π reorganizations during the rotation of the pentadienyl ligands. The calculated bond indices for the various conformations of **1** should be compared with the corresponding values in ferrocene. In the framework of the INDO model a FeC index of 0.2807 and a CC index of 1.3038 are predicted. Stronger FeC interactions therefore are encountered in the open ferrocenes. The origin for these enhanced interactions have been discussed in detail. The mean value of the five Wiberg indices in **1a** (0.2926) exceeds the coupling strength in ferrocene. The collected Wiberg indices clearly display that all VB structures displayed (A, B, A′) contribute to the ground state of the open

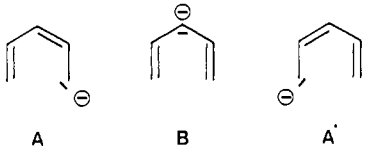

ferrocenes. The enhanced indices at the terminal bonds can be traced to the fact that in A/A′ always a terminal and a central CC bond are strengthened while in B only the terminal bonds are enhanced. In Figure 5 the MO's of **1a** are correlated with the orbital energies of the three methyl derivatives **2**, **3**, and **4**. In Table V additionally the SCF eigenvalues, ϵ_i, of the trans complexes **1a**, **2a**, **3a**, and **4a** are summarized. The alkyl-induced destabilization of the MO's with large π amplitudes is obvious. The Wiberg bond indices of **1a**, **2a**, **3a**, and **4a** are compared in Figure 6. It is seen that alkyl substitution is only of minor

Table V. Comparison between the High-Lying Occupied Valence Orbitals in the Trans-Coordinated Bis(pentadienyl)iron Derivatives 1a, **2a**, 3a, and 4a According to the INDO Method[a]

	ϵ_i			
Γ_i	1a	2a	3a	4a
$8b_u$	−8.17	−7.94	−8.07	−7.91
$10a_g$	−10.56	−10.32	−10.31	−10.20
$7b_g$	−10.62	−10.45	−10.34	−10.31
$6a_u$	−10.79	−10.69	−10.35	−10.32
$9a_g$	−11.13	−10.92	−10.86	−10.79
$8a_g$	−11.29	−11.10	−11.01	−10.97
$6b_g$	−11.32	−11.15	−11.05	−11.04
$7b_u$	−11.43	−10.72	−10.82	−10.59

[a] The irreducible representations correspond to the unsubstituted complex 1a. All values in eV.

Table VI. Comparison between the INDO AO Populations at the 3d Center in 1a and **5**

AO	1a	5
4s	0.088	0.091
$4p_x$	0.042	0.041
$4p_y$	0.051	0.041
$4p_z$	0.057	0.061
$3d_{z^2}$	1.994	1.993
$3d_{xz}$	1.199	0.811
$3d_{yz}$	0.807	0.811
$3d_{x^2-y^2}$	1.663	1.867
$3d_{xy}$	1.665	1.867

Table VII. Comparison between the INDO Net Charges in **1a** and **5**

	net charge		net charge
		1a	
Fe	0.434	H_i=H_5 (endo)	0.178
C_1=C_5	−0.478	H_i=H_5 (exo)	0.124
C_2=C_4	0.033	H_2=H_4	0.117
C_3	−0.312	H_3	0.145
		5a	
Fe	0.416	H	0.132
C	−0.173		

(41) K. B. Wiberg, *Tetrahedron*, **24**, 1083 (1968).
(42) M. Tsutsui and A. Courtney, *Adv. Organomet. Chem.*, **16**, 241 (1979).

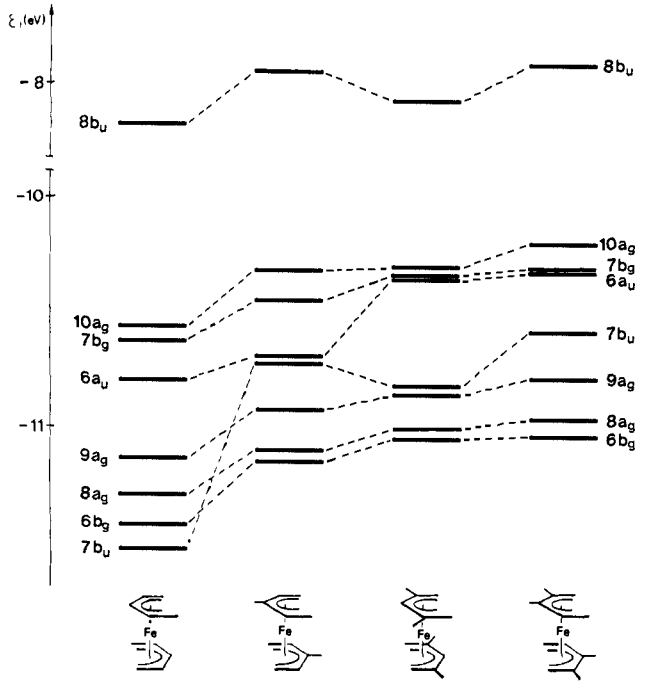

Figure 5. Comparison of the orbital energies in the series **1a**, **2a**, **3a**, and **4a**. The numbering scheme of the irreducible representations corresponds to **1a**.

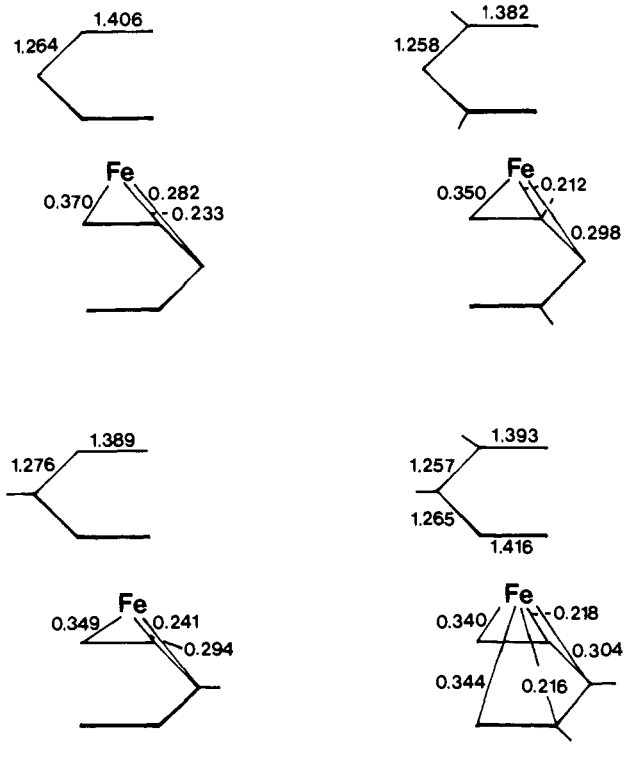

Figure 6. Comparison of the Wiberg indices in the series **1a**, **2a**, **3a**, and **4a**.

importance for the nature of the iron–carbon interaction. A small leveling of the FeC and CC bond indices in the methyl compounds is experienced. However, a secondary influence of the methyl groups in decreasing the interior C–C–C bond angle around the carbon atom to which they are attached may bring about some stabilization due to an increase in metal–ligand overlap. The differences in the bonding capabilities of the open ferrocenes and their closed counterpart **5** can additionally be verified by the INDO AO populations for the iron centers in **1a** and **5** summarized in Table VI as well as on the basis of the Fe and carbon net charges (**1a** and **5**) collected in Table VII. It is seen that the net distribution of the valence electrons between the 3d center and the ligand moieties is of comparable magnitude in both complexes. The difference between the two metallocenes thus lies in different internal (intrametal, intraligand) charge distributions. With respect to the 3d AO population this already has been discussed. The charge accumulation at C_1, C_3, and C_5 in the pentadienyl moieties of **1a** is in line with the displayed VB structures A. B. and A′.

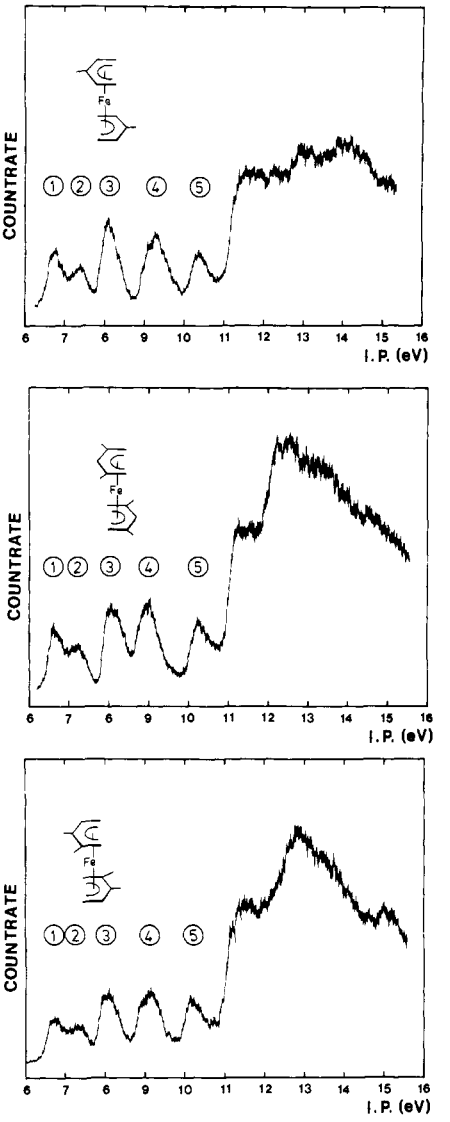

Figure 7. He I PE spectra of **2**, **3**, and **4**.

The He I PE Spectra of 2–4

(a) Qualitative Assignment. In Figure 7 the He I PE spectra of **2–4** are shown. The measured vertical ionization potentials, $I_{v,j}^{expt}$, are collected in Table VIII. The parent compound **1** could not be investigated as the complex is not stable under the conditions employed.

The PE spectra of **2–4** exhibit five band maxima below 11 eV. The intensity of bands 2, 3, 4, and 5 (band numbers are circled in Figure 7) in all three spectra suggest that these bands result from one (bands 2 and 5) or two (bands 3 and 4) ionization events. For the first band the existence of two ionization events with lower intensity seems reasonable.

The relatively strong variation of band 4 as a function of methyl substitution is a hint for ionization processes out of molecular orbitals strongly localized on the ligands.

Our qualitative assignment is confirmed by considering the PE spectrum of ferrocene. In this compound the first two ionization potentials (at 6.86 and 7.23 eV) are assigned to the degenerate molecular orbitals $3d_{x^2-y^2}/3d_{xy}$ and to the $3d_{z^2}$ orbital.[43] The center

Table VIII. Vertical Ionization Potentials, $I_{v,j}^{exptl}$, for the Bis(pentadienyl)iron Derivatives 2–4[a]

peak	2	3	4
1	6.8	6.6	6.6
2	7.4	7.2	7.3
3	8.1	8.0	8.0
4	9.3	8.9	9.0
5	10.3	10.2	10.1

[a] All values in eV.

of gravity of the resulting two bands in **5** is found at 6.98 eV. Recently it has been shown that the lowering of the Fe 3d IP's due to methyl substitution is additive.[44] The shift of the first IP on going from **5** to 1,1'-dimethylferrocene amounts 0.2 eV (center of gravity 6.78 eV). Two additional methyl groups drop this value to 6.58 eV.

In bis(butadiene)iron monocarbonyl (**6**) one ionization event was found, corresponding to an electron ejection from a molecular orbital with a large Fe 3d amplitude (93%).[15] The vertical ionization potential of this process was found to be 6.95 eV. Dialkyl substituents in the diene moiety lower this value to 6.53 eV.[15]

A comparison with the first bands in the PE spectrum of **5** and **6** suggests that the first band in **2–4** corresponds to ionization events with predominant Fe 3d character. In the case of the trans conformers **2a–4a** two such ionization events are expected. Consequently the second peak in **2–4** must be assigned as due to the ejection from the nonbonding pentadienyl MO.

The complexes **2–4** differ from the bis(π-allyl)nickel derivatives with respect to the sequence of the first two PE bands. In the nickel complexes the first band has been assigned to the nonbonding ligand MO.[13,24] Intensity arguments are also in line with the assignment just discussed for bands 1 and 2 of **2** to **4**. Below we have collected the corrected[45] integrated band intensities for bands 1 to 5 of **2–4** using band 2 as an internal standard.

2	band	1	2	3	4	5
	rel intensity	1.2	1.0	1.6	1.7	1.0
3	band	1	2	3	4	5
	rel intensity	1.2	1.0	1.7	1.7	1.1
4	band	1	2	3	4	5
	rel intensity	1.2	1.0	1.6	1.8	1.2

In **5** an intensity ratio between an ionization event from a metal 3d orbital and from a ligand π-orbital is found of 0.60 to 0.62[43,44]). Thus if bands 2 and 5 correspond to one ligand ionization process, the intensity of band 1 is in line with two transitions from orbitals with large Fe 3d amplitudes. Bands 3 and 1 of **2–4** with about equal intensities ($\sim$1.7) must be assigned to two ionization events. The reduced cross sections—compared with those of bands 2 and 5—indicate remarkable Fe 3d contributions to the corresponding molecular orbitals. In the absence of iron 3d contributions to the orbital wave function approximate intensity ratios of 2:1 must be expected for bands 1 and 5 on one side and bands 3 and 4 on the other. The reduced cross sections hence can only be the result of ionization processes out of MO's with significant Fe 3d amplitudes (see also ref 44).

If we assume the trans conformation for **2–4**, the results in Tables V and VIII suggest the following assignment. Band 1 corresponds to electron ejections from the Fe 3d molecular orbitals $9a_g$ and $8a_g$, and band 2 is assigned to the HOMO ($8b_u$). Band 5 is assigned due to the ionization from the third ungerade linear combination $7b_u$. Significant reorganization effects must be expected in the case of $7b_g$, $10a_g$, and $6b_g$ since Fe 3d contributions

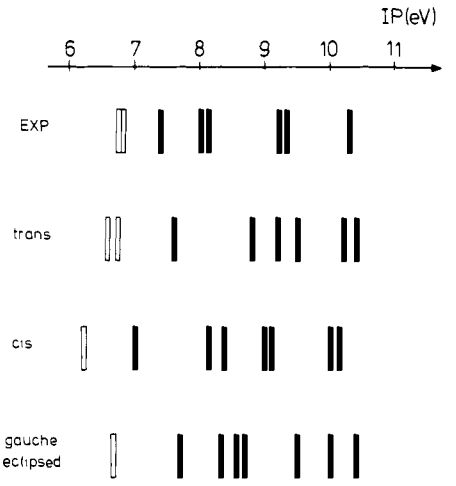

Figure 8. Comparison between the measured vertical IP's of **2** and calculated ones (according to the inverse Dyson equation) for the trans, cis, and gauche-eclipsed conformations. The full (open) bars represent those molecular orbitals with a strong ligand (3d) character.

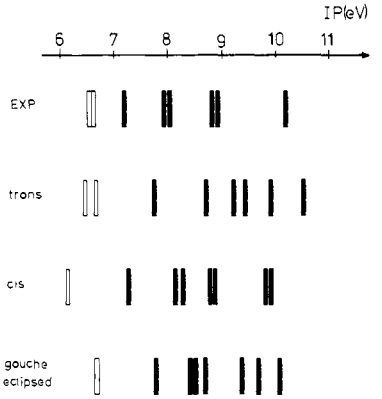

Figure 9. Comparison between the measured vertical IP's of **3** and calculated ones (according to the inverse Dyson equation) for the trans, cis, and gauche-eclipsed conformations. The full (open) bars represent those molecular orbitals with a strong ligand (3d) character.

between 35% and 45% are predicted for these molecular orbitals. Based on our previous experience,[13,14,23,24] we assign tentatively band 3 to ionization events from $7b_g$ and $10a_g$ and band 4 to events from $6a_u$ and $6b_g$.

(b) Calculation of Ionization Potentials. Since all three PE spectra (**2–4**) are very similar (see Figure 7), we have carried out calculations using Green's function technique only on **2** and **3**. We have selected the trans (C_{2h}), cis (C_{2v}), and the gauche-eclipsed conformations. For the determination of the self-energy operator 13 hole states and 10 particle functions were taken into account.

In Figures 8 and 9 the experimental ionization potentials, $I_{v,j}^{exptl}$, of **2** and **3** are compared with theoretical ionization potentials derived by means of the inverse Dyson equation. It is seen that the ionization potentials calculated for the trans C_{2h} conformation (**2a** and **3a**) are closest to the measured ionization energies. This indicates that the gas-phase geometry of the bis(pentadienyl)iron compounds corresponds to the predicted C_{2h} minimum (see Ground-State Properties). On the basis of the splitting pattern of Figures 8 and 9 the cis C_{2v} conformation cannot be ruled out. The energy gaps between the various bands are also in line with the measured differences of the various IP's. On the other hand the C_{2v} conformation unambiguously can be excluded on the basis of the intensity arguments that already have been discussed in some detail and on the basis of the center of gravity for the "3d" IP's in ferrocene. Thus the trans arrangement of the open ferrocenes is the only conformation where both the sequence of the measured IP's and the expected cross sections (derived from the composition of the orbital wave functions) are in line with the experimental data.

(43) S. Evans, A. F. Orchard, and D. W. Turner, *Int. J. Mass. Spectrom. Ion Phys.*, 7, 261 (1971); J. W. Rabalais, L. O. Werme, T. Bergmark, L. Karlson, M. Hussain, and K. Siegbahn, *J. Chem. Phys.*, **57**, 1185 (1972); S. Evans, M. L. H. Green, B. Jewitt, A. F. Orchard, and C. F. Pygall, *J. Chem. Soc., Faraday Trans. 2* **68**, 1847 (1972).

(44) C. Cauletti, J. C. Green, M. R. Kelly, P. Powell, J. van Tilborg, J. Robbins, and J. Smart, *J. Electron Spectrosc. Relat. Phenom.*, **19**, 327 (1980).

(45) $I_{corr} = I_{measd}(21.4 - I_{v,j}^{exptl})$. In ref 46 the wrong proportionality between the corrected intensities and the influence of the energy of the photoejected electrons is given.

(46) C. D. Batich, *J. Am. Chem. Soc.*, **98**, 7585 (1976).

Table IX. Comparison between the Experimentally Determined Vertical Ionization Potentials, $I_{v,j}^{exptl}$, of **2** and **3** and the Calculated Ones. Assuming the Validity of Koopmans' Theorem, $I_{v,j}^{K}$, and Using the Inverse Dyson Equation ($I_{v,j}^{K} + \Sigma_{jj}^{(2)}(\omega_j)$)[a]

peak	Γ_j	MO	$I_{v,j}^{K}$	$I_{v,j}^{K} + \Sigma_{jj}^{(2)}(\omega_j)$	$I_{v,j}^{exptl}$
			2		
1	$8a_g$	31	11.10	6.57	6.8
	$9a_g$	32	10.92	6.77	
2	$8b_u$	37	7.94	7.64	7.4
3	$7b_g$	35	10.45	8.84	8.1
	$10a_g$	36	10.32	9.24	
4	$6b_g$	30	11.15	9.52	9.3
	$6a_u$	34	10.69	10.27	
5	$7b_u$	33	10.72	10.41	10.3
			3		
1	$8a_g$	37	11.01	6.48	6.6
	$9a_g$	38	10.82	6.71	
2	$8b_u$	43	8.07	7.77	7.2
3	$7b_g$	41	10.34	8.73	8.0
	$10a_g$	42	10.32	9.24	
4	$6b_g$	36	11.05	9.42	8.9
	$6a_u$	40	10.35	9.93	
5	$7b_u$	39	10.82	10.51	10.2

[a] All values in eV.

In Table IX the experimentally determined vertical ionization potentials, $I_{v,j}^{exptl}$, of **2** and **3** are compared with calculated ionization potentials for the trans conformation (**2a** and **3a**), assuming the validity of Koopmans' theorem, $I_{v,j}^{K}$, and using the inverse Dyson equation (9). A graphical representation of this comparison for **2** is given in Figure 10. It is seen that both PE spectra are well reproduced by Green's function approach. The largest reorganization effects are encountered in the case of the strongly localized molecular orbitals $9a_g$ and $8a_g$. Deviations from $I_{v,j}^{K}$ exceeding 4 eV are responsible for the dramatical breakdown of the Koopmans' configurations. Significant orbital reorganization is also calculated for the molecular orbitals $7b_g$, $10a_g$, and $6b_g$ where comparable contributions from the ligands and the 3d center to the one-electron wave functions are calculated. The observed Koopmans' defects are about 1.3–2.0 eV. In the case of the MO's with ungerade symmetry, i.e., MO's which do not interact with Fe 3d AO's, only small deviations from $I_{v,j}^{K}$ are computed (less than 0.5 eV).

The results of Table IX and Figure 10 indicate that the ionization events of the bis(pentadienyl)iron complexes can be separated into three classes. Koopmans' theorem is valid for ionization processes from pure ligand orbitals. Strong reorganization effects are found in the case of the two "Fe 3d" MO's $9a_g$ and $8a_g$. This defect pattern has been detected also in ΔSCF[9,10,14] and the many-body perturbation theoretical[47] calculations for ferrocene. In contrast to the cyclic 3d metallocene, strong metal-to-ligand coupling in the open ferrocenes leads to a third group of orbitals with comparable metal and ligand character. The predicted Koopmans' defects for this class of molecular orbitals lie between the reorganization energies of the localized 3d orbitals and the small deviations of the pure ligand functions as anticipated.

The INDO results summarized in Figure 10 indicate that the semiempirical LCAO method in connection with the many-body perturbation theory predicts vertical ionization potentials with remarkable accuracy. The absolute values of the ionization energies, the energy gap between the various bands, and the near degeneracy of always two ionization events in bands 1, 3, and 4 are well reproduced by the computational procedure.

Final Remarks

The electronic structure of a series of open ferrocenes has been investigated by means of semiempirical MO calculations and by means of their He I PE spectra and has been compared with ferrocene. Due to the larger flexibility of the Fe 3d set in C_{2h} symmetry an enhanced δ coupling between the Fe center and the pentadienyl ligands has been encountered. The discussion in Ground-State Properties however, has demonstrated that this nomenclature must be used with some care. The overall charge distribution in the open systems is comparable to the ferrocene case; differences, however, are predicted for individual Fe 3d AO's or carbon centers in the pentadienyl ligands (in comparison to the Cp frame). The bonding interactions in **1a** deduced from INDO calculations are in good agreement with recent Mössbauer studies. Significant differences between the open systems and **5** are also predicted with respect to the ionization pattern of the Fe complexes. In ferrocene, model calculations predict three molecular orbitals with predominant Fe 3d character ($3d_{z^2}$, $3d_{x^2-y^2}$, and $3d_{xy}$). In the open ferrocenes investigated in this work $3d_{xy}$ is found to be strongly coupled to ligand functions and only $3d_{z^2}$ and $3d_{x^2-y^2}$ are strongly localized on the metal. In the bis(diene)iron monocarbonyl series only a single molecular orbital with predominant Fe 3d character is found since two components of the three 3d orbitals, $3d_{z^2}$, $3d_{x^2-y^2}$, and $3d_{xy}$, interact significantly with fragment orbitals of the ligands (diene, CO). The same interaction pattern is also predicted for those conformations of bis(pentadienyl)iron which deflect from the trans (C_{2h}) conformation. These different localization properties for the MO's with large Fe 3d contributions lead to PE spectra that differ remarkably.

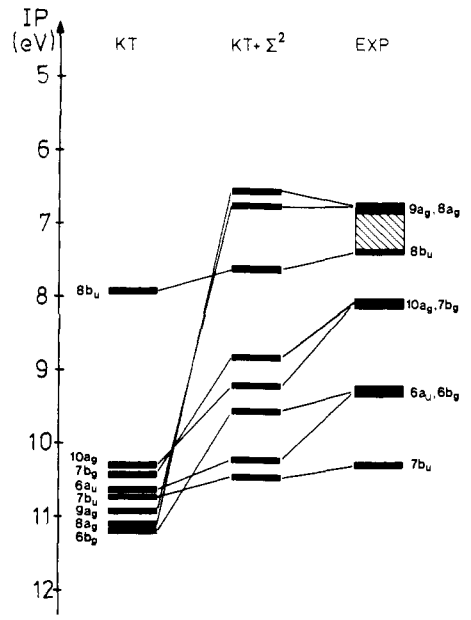

Figure 10. Comparison between the first peaks in the PE spectrum of **2**(EXP) with the calculated ionization energies assuming the validity of Koopmans' theorem (KT) and using the inverse Dyson equation (K + Σ^2). All calculations were performed for the trans C_{2h} arrangement of the pentadienyl ligands.

Experimental Section

The preparation of **2**, **3** and **4** has been described in the literature.[5] The He I PE spectra were measured on a PS 18 instrument of Perkin-Elmer Ltd. (Beaconsfield, England) and were calibrated with Ar. A resolution of about 20 meV of the $^2P_{3/2}$ Ar line was obtained.

Acknowledgment. The work at Heidelberg has been supported by the Stiftung Volkswagenwerk, by the Fonds der Chemischen Industrie, and by the BASF in Ludwigshafen. The work at Utah has been supported through grants from the donors of the Petroleum Research Fund, administered by the American Chemical Society, and from the University of Utah Research Committee. R.D.E. and R.G. are grateful to NATO for a travel-grant.

Registry No. 1, 74910-62-6; **2**, 74910-63-7; **3**, 74920-98-2; **4**, 74910-64-8.

(47) M. C. Böhm and R. Gleiter, in preparation.